



## RESEARCH LETTER

10.1002/2016GL069239

## Key Points:

- Particulate organic nitrate is ubiquitous in Europe
- The 34 to 44 percent of fine particulate nitrate is organic
- Nighttime chemistry is a dominant source of particulate organic nitrates

## Supporting Information:

- Supporting Information S1
- Supporting Information S2

## Correspondence to:

A. Kiendler-Scharr,  
a.kiendler-scharr@fz-juelich.de

## Citation:

Kiendler-Scharr, A., et al. (2016), Ubiquity of organic nitrates from nighttime chemistry in the European submicron aerosol, *Geophys. Res. Lett.*, *43*, 7735–7744, doi:10.1002/2016GL069239.

Received 18 APR 2016

Accepted 9 JUL 2016

Accepted article online 13 JUL 2016

Published online 30 JUL 2016

## Ubiquity of organic nitrates from nighttime chemistry in the European submicron aerosol

A. Kiendler-Scharr<sup>1</sup>, A. A. Mensah<sup>1,2</sup>, E. Friese<sup>3</sup>, D. Topping<sup>4,5</sup>, E. Nemitz<sup>6</sup>, A. S. H. Prevot<sup>7</sup>, M. Äijälä<sup>8</sup>, J. Allan<sup>4,5</sup>, F. Canonaco<sup>7</sup>, M. Canagaratna<sup>9</sup>, S. Carbone<sup>10,11</sup>, M. Crippa<sup>7,12</sup>, M. Dall'Osto<sup>13</sup>, D. A. Day<sup>14</sup>, P. De Carlo<sup>7</sup>, C. F. Di Marco<sup>6</sup>, H. Elbern<sup>3</sup>, A. Eriksson<sup>15</sup>, E. Freney<sup>16</sup>, L. Hao<sup>17</sup>, H. Herrmann<sup>18</sup>, L. Hildebrandt<sup>19</sup>, R. Hillamo<sup>10</sup>, J. L. Jimenez<sup>14</sup>, A. Laaksonen<sup>8,17</sup>, G. McFiggans<sup>4</sup>, C. Mohr<sup>7,20</sup>, C. O'Dowd<sup>13</sup>, R. Otjes<sup>21</sup>, J. Ovadnevaite<sup>13</sup>, S. N. Pandis<sup>22</sup>, L. Poulain<sup>18</sup>, P. Schlag<sup>1</sup>, K. Sellegri<sup>16</sup>, E. Swietlicki<sup>15</sup>, P. Tiitta<sup>17</sup>, A. Vermeulen<sup>21</sup>, A. Wahner<sup>1</sup>, D. Worsnop<sup>9</sup>, and H.-C. Wu<sup>1</sup>

<sup>1</sup>IEK-8: Troposphäre, Forschungszentrum Jülich GmbH, Jülich, Germany, <sup>2</sup>Now at Institut für Atmosphäre und Klima, ETH Zürich, Zürich, Switzerland, <sup>3</sup>Rhenish Institute for Environmental Research, University of Cologne, Cologne, Germany, <sup>4</sup>School of Earth, Atmospheric and Environmental Sciences, University of Manchester, Manchester, UK, <sup>5</sup>National Centre for Atmospheric Science, University of Manchester, Manchester, UK, <sup>6</sup>Centre for Ecology and Hydrology, Penicuik, UK, <sup>7</sup>Paul Scherrer Institute, Villigen, Switzerland, <sup>8</sup>Department of Physics, Helsinki University, Helsinki, Finland, <sup>9</sup>Aerodyne Research Inc., Billerica, Massachusetts, USA, <sup>10</sup>Finnish Meteorological Institute, Helsinki, Finland, <sup>11</sup>Now at IAG, University of São Paulo, São Paulo, Brazil, <sup>12</sup>Now at EC Joint Research Centre, Institution Environment and Sustainability, Ispra, Italy, <sup>13</sup>School of Physics, National University of Ireland Galway, Galway, Ireland, <sup>14</sup>Cooperative Institute for Research in Environmental Sciences and Department of Chemistry and Biochemistry, University of Colorado Boulder, Boulder, Colorado, USA, <sup>15</sup>Department of Physics, Lund University, Lund, Sweden, <sup>16</sup>Laboratoire de Météorologie Physique, CNRS-Université Blaise Pascal, Clermont Ferrand, France, <sup>17</sup>Department of Applied Physics, University of Eastern Finland, Kuopio, Finland, <sup>18</sup>Leibniz Institute for Tropospheric Research, Leipzig, Germany, <sup>19</sup>McKetta Department of Chemical Engineering, University of Texas at Austin, Austin, Texas, USA, <sup>20</sup>Now at Institute of Meteorology and Climate Research, Karlsruhe Institute of Technology, Karlsruhe, Germany, <sup>21</sup>Energy Research Centre of the Netherlands, Petten, Netherlands, <sup>22</sup>Department of Chemical Engineering, University of Patras, Patras, Greece

**Abstract** In the atmosphere nighttime removal of volatile organic compounds is initiated to a large extent by reaction with the nitrate radical (NO<sub>3</sub>) forming organic nitrates which partition between gas and particulate phase. Here we show based on particle phase measurements performed at a suburban site in the Netherlands that organic nitrates contribute substantially to particulate nitrate and organic mass. Comparisons with a chemistry transport model indicate that most of the measured particulate organic nitrates are formed by NO<sub>3</sub> oxidation. Using aerosol composition data from three intensive observation periods at numerous measurement sites across Europe, we conclude that organic nitrates are a considerable fraction of fine particulate matter (PM<sub>1</sub>) at the continental scale. Organic nitrates represent 34% to 44% of measured submicron aerosol nitrate and are found at all urban and rural sites, implying a substantial potential of PM reduction by NO<sub>x</sub> emission control.

### 1. Introduction

Atmospheric self-cleansing, i.e., removal of species through oxidation, is initiated by the radical species OH, O<sub>3</sub>, and NO<sub>3</sub>. While OH plays a key role during the day and is overall the dominant oxidant in the troposphere, NO<sub>3</sub> is one of the main oxidants during the night in addition to O<sub>3</sub>. Due to its formation from the reaction of NO<sub>2</sub> with O<sub>3</sub> the main source of NO<sub>3</sub> is anthropogenic. Already in 1984 it was suggested that the reaction with NO<sub>3</sub> radicals is a dominant loss process for monoterpenes [Winer *et al.*, 1984]. Especially emissions that remain in the atmosphere at sunset or enter in the night undergo oxidation by NO<sub>3</sub> radicals [Pye *et al.*, 2010]. Model estimates conclude that 6–20% of the total isoprene emissions are oxidized by NO<sub>3</sub> [Brown *et al.*, 2009]. Oxidation of VOCs leads to either functionalization or fragmentation of precursor molecules, where fragmentation likely leads to products with higher vapor pressure than the precursors' vapor pressure. By contrast, functionalization results in a decrease of the vapor pressure [Pankow and Asher, 2008], which in the case of NO<sub>3</sub> radical reactions is dominated by addition reactions forming multifunctional nitrates (RONO<sub>2</sub>). Products with low enough vapor pressures will partition to the particulate phase, forming secondary organic aerosol (SOA) and thereby contribute to air quality and climate impacts of particles.

While the formation of SOA through VOC oxidation by OH and O<sub>3</sub> has been studied in numerous simulation chamber and laboratory experiments [Hallquist *et al.*, 2009], only few experiments report the SOA yields from the oxidation with NO<sub>3</sub> [e.g., Boyd *et al.*, 2015; Brown and Stutz, 2012; Fry *et al.*, 2014]. For the biogenic VOCs investigated, SOA yields vary between 1 and 89% and RONO<sub>2</sub> yields between 19 and 66%. These reactions have also been shown to result in a substantial fraction (12 to 16%) of the oxidized nitrogen consumed by biogenic VOC oxidation in some continental regions [Brown *et al.*, 2009].

Observations of ambient atmospheric particles have shown that organic species are ubiquitous and represent a large fraction of observed mass loadings regardless of location of the measurement [Zhang *et al.*, 2007]. Recent attempts to model the organic aerosol (OA) mass have substantially improved the ability of models to reproduce measured organic mass loadings, yet large uncertainties remain with respect to OA sources [Hallquist *et al.*, 2009]. For instance, it has been shown using radiocarbon measurements that a major part of the OA mass is of modern origin in many areas, meaning that sources such as biogenic VOC and biomass burning are often dominant sources of OA [e.g., Szidat *et al.*, 2006]. Nevertheless, SOA is often observed to correlate well with gas-phase tracers for anthropogenic activity such as carbon monoxide (CO) [Weber *et al.*, 2007], and recent model results suggest that interactions of anthropogenic pollution and biogenic VOCs (BVOCs) may be important on a global scale [Spracklen *et al.*, 2011]. A prominent candidate for production of aerosol from modern carbon that would correlate with anthropogenic tracers is the reaction of NO<sub>3</sub> with BVOCs, which has been shown to serve as source of particulate organic nitrates in recent studies in the U.S. [Fry *et al.*, 2013; Rollins *et al.*, 2012; Setyan *et al.*, 2012; Xu *et al.*, 2015a, 2015b].

Here we present evidence from aerosol mass spectrometric (AMS) measurements with high time resolution that, in urban and rural sites in Europe, the reaction of VOCs with nitrate radicals represents an important source of OA.

## 2. Materials and Methods

Intensive AMS measurements were taken across Europe through three campaigns within the European Integrated Project on Aerosol Cloud Climate and Air Quality Interactions (EUCAARI)/European Monitoring and Evaluation Programme (EMEP) intensives in May 2008, October 2008, and March 2009 [Crippa *et al.*, 2013; Kulmala *et al.*, 2011]. Observations were compared with results from the European Air pollution and Dispersion-Inverse Model (EURAD-IM) chemistry transport model [Elbern *et al.*, 2007] in order to evaluate the regional extent of our findings. Here we discuss the data analysis principles applied to derive organic nitrate mass concentration from AMS data and the setup of the EURAD-IM used for comparing to the measurement episodes.

### 2.1. AMS Data Analysis for Organic Nitrate

The working principles and modes of operation of the aerosol mass spectrometer (AMS) are described in detail elsewhere [Canagaratna *et al.*, 2007]. Here we report on the method used to quantify the organic nitrate in the measured total nitrate. In AMS measurements nitrate is primarily quantified by the determination of the total signal of NO<sub>2</sub><sup>+</sup> and NO<sup>+</sup> (high-resolution time-of-flight version, HR-TOF-AMS [DeCarlo *et al.*, 2006]) or the signal at *m/z* 30 and *m/z* 46 that is attributed to nitrate via the so-called fragmentation table (quadrupole aerosol mass spectrometer, Q-AMS [Jayne *et al.*, 2000]). Ambiguity remains for the Q-AMS data sets due to the correction of the interference of the CH<sub>2</sub>O<sup>+</sup> ion at *m/z* 30, whereas *m/z* 46 is traditionally interpreted as being dominated by NO<sub>2</sub><sup>+</sup> [Allan *et al.*, 2004]. By contrast, the HR-TOF-AMS can unambiguously distinguish between the NO<sup>+</sup> and CH<sub>2</sub>O<sup>+</sup> ions (see Table S1 in the supporting information for an overview of stations and AMS type applied).

The measured ratio of NO<sub>2</sub><sup>+</sup>/NO<sup>+</sup> was taken from all AMS data sets to determine the fractional contribution of ammonium nitrate (NH<sub>4</sub>NO<sub>3</sub>, hereafter plnNO<sub>3</sub>) and organic nitrate (pOrgNO<sub>3</sub>) to the total observed signal at these two ions. This requires knowledge of the expected ratio of NO<sub>2</sub><sup>+</sup>/NO<sup>+</sup> for pure ammonium nitrate and pure organic nitrate. As calibrations of the ionization efficiency of the AMS are typically performed with NH<sub>4</sub>NO<sub>3</sub> particles, the measured ratio of NO<sub>2</sub><sup>+</sup>/NO<sup>+</sup> for pure NH<sub>4</sub>NO<sub>3</sub> particles is known for all instruments. Table S1 in the supporting information summarizes the measured calibration ratio *R*<sub>calib</sub> of NO<sub>2</sub><sup>+</sup>/NO<sup>+</sup> for the instruments deployed during the EUCAARI/EMEP intensive observation periods [Crippa *et al.*, 2013; Kulmala *et al.*, 2011]. Note that although there is some variability between instruments, the majority of the instruments report calibration ratios between 0.29 and 0.49 (22 out of 25 instruments). For the remaining

three data sets  $R_{\text{calib}}$  between 0.7 and 0.85 were reported. For organic nitrates literature data suggest a range of possible ratios (0.2 to 0.08) from experiments forming organic nitrates by oxidation of volatile organic compounds (VOCs) with  $\text{NO}_3$  [Boyd *et al.*, 2015; Bruns *et al.*, 2010; Fry *et al.*, 2009, 2011; Rollins *et al.*, 2009]. Here we use a fixed value of  $\text{NO}_2^+/\text{NO}^+$  (i.e., 0.1) for organic nitrates (see also Figures S1 and S2 in the supporting information). This number was chosen as it represents the minimum ratio of  $\text{NO}_2^+/\text{NO}^+$  observed in the field data sets. Note that such low ratios of  $\text{NO}_2^+/\text{NO}^+$  were also detected in some data sets where  $R_{\text{calib}}$  was reported high. Therefore, contrary to other studies, no systematic change in  $R_{\text{OrgNO}_3}$  depending on  $R_{\text{calib}}$  was assumed [Fry *et al.*, 2013]. Our overall approach here is designed such that lower limits of  $\text{pOrgNO}_3$  [Xu *et al.*, 2015a] are derived, with an estimated uncertainty of  $\pm 20\%$ .

Similar to previous attempts to determine the organic nitrate in AMS data sets [Farmer *et al.*, 2010], we apply the following formula to determine the fraction of particulate organic nitrate ( $\text{pOrgNO}_{3\text{frac}}$ ) in the measured total nitrate from measured  $\text{NO}_2^+/\text{NO}^+$  ratio:

$$\text{pOrgNO}_{3\text{frac}} = \frac{(1 + R_{\text{OrgNO}_3}) \times (R_{\text{measured}} - R_{\text{calib}})}{(1 + R_{\text{measured}}) \times (R_{\text{OrgNO}_3} - R_{\text{calib}})} \quad (1)$$

$$\text{pOrgNO}_{3\text{mass}} = \text{pOrgNO}_{3\text{frac}} \times \text{NO}_{3\text{total}} \quad (2)$$

where  $R_{\text{measured}}$  is the measured intensity ratio of  $\text{NO}_2^+$  and  $\text{NO}^+$  ions as function of time in the individual data sets,  $R_{\text{calib}}$  is the ratio observed in  $\text{NH}_4\text{NO}_3$  calibrations, and  $R_{\text{OrgNO}_3}$  is set to 0.1 for all data sets. The mass concentration of  $\text{pOrgNO}_3$  ( $\text{pOrgNO}_{3\text{mass}}$ ) is then calculated by multiplying the measured total nitrate ( $\text{NO}_{3\text{total}}$ ) with the fraction of  $\text{pOrgNO}_3$  (2). Note that since  $\text{NO}_2^+$  is always the ion with less signal intensity, through the use of measured  $\text{NO}_2^+/\text{NO}^+$  ratio rather than  $\text{NO}^+/\text{NO}_2^+$  ratio, we are using a formulation that approaches zero in the case of very low or nonexistent signal, whereas the use of  $\text{NO}^+/\text{NO}_2^+$  ratio gives infinite numbers as the limit of detection is approached.

Note that the  $\text{pOrgNO}_3$  calculated this way accounts for the nitrate functional group of organic nitrates only. This method was previously considered to reliably derive the  $\text{pOrgNO}_3$  fraction when  $\text{pOrgNO}_{3\text{frac}}$  is  $>0.15$  [Bruns *et al.*, 2010]. Therefore, organic nitrate concentration data reported here were filtered for values  $>0.15$ . Also, in a conservative approach [Bruns *et al.*, 2010] we consider  $0.1 \mu\text{g m}^{-3}$   $\text{pOrgNO}_3$  as detection limit and report data accordingly.

## 2.2. EURAD-IM Model Description

The EURAD-IM [Elbern *et al.*, 2007], is a Eulerian model running from local to continental scale. EURAD-IM is primarily used for chemical weather forecast and advanced data assimilation studies over Europe, using the RACM chemistry mechanism [Stockwell *et al.*, 1997]. Previous studies on a high-ozone episode [Monteiro *et al.*, 2012] and a dust storm [Chervakov and Jakobs, 2011] indicated good performances of EURAD-IM. Within EURAD-IM, the aerosol dynamics such as nucleation, condensation, coagulation, diffusion, sedimentation, and aerosol-cloud interaction are simulated by the Modal Aerosol Dynamics Model for Europe (MADE [Ackermann *et al.*, 1998]). However, the initial MADE aerosol chemistry module only treated inorganic ions and water. To consider the formation of secondary organic aerosols, the Secondary ORGANic Aerosol Model (SORGAM) was developed and implemented into MADE [Schell *et al.*, 2001]. In SORGAM, both anthropogenic and biogenic hydrocarbons are first oxidized by oxidants like OH,  $\text{NO}_3$ , and  $\text{O}_3$ . The mass transfer from gas to particle phase is then driven by the gas/particle partitioning of the low-volatility oxidation products formed in gas phase. Aerosol dry deposition velocities are calculated according to Zhang *et al.* [2003]. Recently, it was shown that including SOA formation from  $\text{NO}_3$  oxidation significantly improved the ability to model OOA at Cabauw, the Netherlands [Li *et al.*, 2013]. EURAD-IM is part of the MACC II (Monitoring Atmospheric Composition and Climate - Interim Implementation) consortium and, together with six other CTMs, operated and evaluated on a daily basis (<http://www.gmes-atmosphere.eu/documents/maccii/deliverables/eva>, 2013, 2013). It was found that especially  $\text{NO}_2$  analyses performed very well.

In this study EURAD-IM was used with a spatial resolution of 15 km with improvements in the SOA scheme as described in Li *et al.* [2013]. Recently, Model of Emissions of Gases and Aerosols from Nature (MEGAN) 2.1 [Guenther *et al.*, 2012] has been implemented into EURAD-IM and was used for the calculation of biogenic emissions in this study. Anthropogenic emissions have been derived from the MACC-II TNO (Netherlands Organisation for Applied Scientific Research) emission inventory for the year 2009 [Pouliot *et al.*, 2012]. The

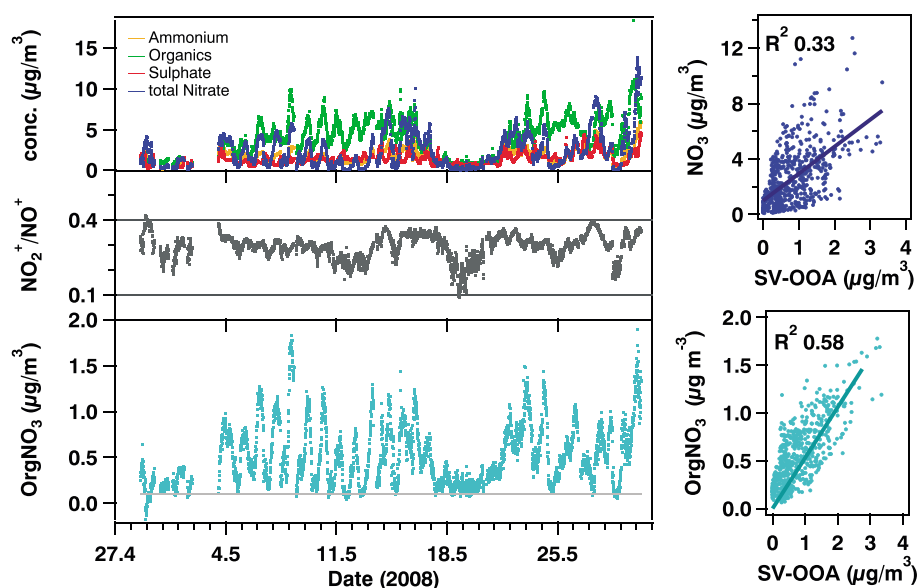


**Figure 1.** Measured mass concentrations of ammonium (orange), total nitrate (dark blue), sulphate (red), and organics (green) together with observed concentration ratio of  $\text{NO}_2^+/\text{NO}^+$  ions (dark grey) and organic nitrate (pOrgNO<sub>3</sub>, cyan) mass concentration at Cabauw, the Netherlands. Also shown are correlations of the SV-OOA factor with total nitrate (top right) and organic nitrate (bottom right).

Weather Research and Forecasting Model V3.5, driven by the Integrated Forecasting System operational analysis, has been used for the provision of meteorological fields needed by EURAD-IM. The comparison of model output with measurements presented in the following focuses on SOA formed through NO<sub>3</sub> oxidation.

### 3. Organic Nitrate Results From Cabauw Analysis

Figure 1 shows observed mass concentrations of the submicron nonrefractory aerosol species ammonium (orange), organics (green), sulphate (red), and total nitrate (blue) as measured with a HR-ToF-AMS at Cabauw, the Netherlands, in May 2008 [Mensah *et al.*, 2012]. Using the observed intensity ratio of the ions NO<sub>2</sub><sup>+</sup> and NO<sup>+</sup> (middle of Figure 1) to calculate the relative contribution of nitrate groups associated with either pOrgNO<sub>3</sub> or pInNO<sub>3</sub> to the measured total aerosol nitrate (pNO<sub>3</sub>), we infer a pOrgNO<sub>3</sub> mass concentration averaging 0.52 µg m<sup>-3</sup> and as high as 1.8 µg m<sup>-3</sup>.

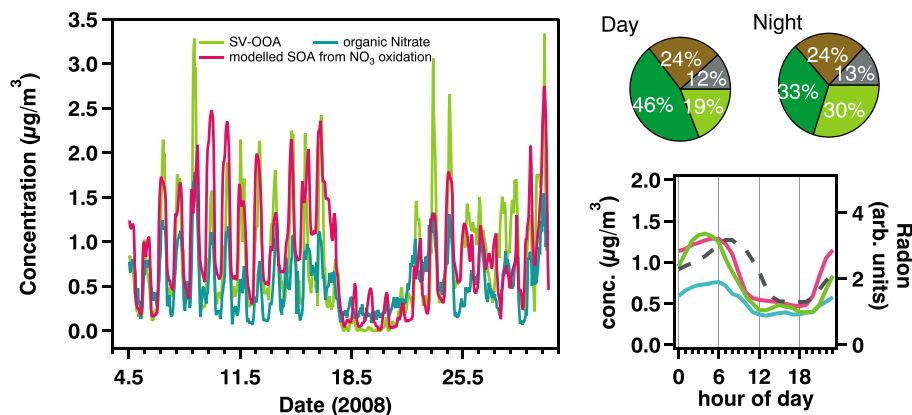


**Figure 2.** Time series of the mass concentrations of measured organic nitrate and SV-OOA and modeled SOA from NO<sub>3</sub> oxidation at Cabauw during May 2008. Inserts show the average diurnal including also Radon concentration (grey dashed line, right axis) as boundary layer dilution tracer and day and night pie charts of the relative contribution of individual organic PMF factors.

The time series of pOrgNO<sub>3</sub> is characterized by a distinct diurnal pattern with maxima during the night (see also Figure 2) and is correlated ( $R^2 = 0.58$ ) with the less oxidized fraction of the oxidized OA (SV-OOA), as determined by positive matrix factorization (PMF [Ulbrich *et al.*, 2009]) and a unified multilinear engine (ME-2) analysis for all EUCAARI/EMEP data sets [Crippa *et al.*, 2013; Paglione *et al.*, 2014]. Note that this correlation between pOrgNO<sub>3</sub> and SV-OOA is more pronounced than the correlation of total pNO<sub>3</sub> with SV-OOA.

It has to be emphasized that pOrgNO<sub>3</sub> measures the nitrate functionality of organic nitrates only. To account for the total particulate organic nitrate mass (RONO<sub>2</sub>), an estimate needs to be made regarding the molar mass of RONO<sub>2</sub> relative to molar mass of NO<sub>3</sub>. As a lower limit we will assume a molar mass of 200 g mol<sup>-1</sup> in calculations of the contribution of organic nitrates to total organics [Xu *et al.*, 2015a; Lee *et al.*, 2016].

Using the EURAD-IM model, the SOA formed from oxidation of VOCs by NO<sub>3</sub> was modeled for the measurement period of May 2008 at Cabauw [Li *et al.*, 2013]. As shown in Figure 2, the temporal behavior of the modeled SOA from NO<sub>3</sub> oxidation closely matches the observed SV-OOA and pOrgNO<sub>3</sub> time series. Maximum concentrations are observed for all three at 5:00 LT with a daytime minimum extending from 10:00 to 20:00 LT. For comparison, radon concentration, which can be considered as a tracer for boundary layer dilution, is observed to have a maximum between 7:00 and 8:00 LT, i.e., later than pOrgNO<sub>3</sub>. This is in agreement with a modeled time lag of 2 h between the early morning decrease of SOA from NO<sub>3</sub> oxidation (due to NO<sub>3</sub> photolysis and thus halted production) and the decrease of a dilution tracer (due to breakup of the nocturnal boundary layer) in the EURAD-IM model. Together with a distinct daytime maximum of the photochemically formed sulphate (see Figure S3), we take this comparison as further support that the observed organic nitrate is primarily formed through nighttime NO<sub>3</sub> chemistry.

#### 4. Organic Nitrate Across Europe

Extending the data analysis to the full EUCAARI/EMEP AMS data set [Kulmala *et al.*, 2011], we find that pOrgNO<sub>3</sub> is present throughout Europe (Figure 3) with observed concentrations likely a result of complex interplay of various sources and sinks. Maximum concentrations of pOrgNO<sub>3</sub> are observed for European sites with large anthropogenic influence, i.e., urban (two sites) and rural (nine sites) environments, whereas pOrgNO<sub>3</sub> is very low or below detection limit at the three remote and two high-altitude sites. Averaging over all stations, the fraction of aerosol nitrate that is observed to be pOrgNO<sub>3</sub> showed little variability with values of 34%, 38%, and 44% in March 2009, May 2008, and October 2008, respectively (see Table S1 and S2 in the supporting information for details [Carbone *et al.*, 2014; Dall'Osto *et al.*, 2010; Freney *et al.*, 2011; Hildebrandt *et al.*, 2011; Lanz *et al.*, 2010; Mensah *et al.*, 2012; Minguillón *et al.*, 2011; Mohr *et al.*, 2012; Paglione *et al.*, 2014; Pikridas *et al.*, 2010; Poulain *et al.*, 2011; Saarikoski *et al.*, 2012]). Assuming a molar mass of 200 g mol<sup>-1</sup> for organic nitrates, the mean fractional contribution of organic nitrates to organics was 46% for stations fulfilling the threshold criterion of pOrgNO<sub>3</sub> > 0.1 μg m<sup>-3</sup> (18 out of 25 data sets). Note that this is equivalent to a contribution of organic nitrates to nonrefractory PM1 of between 5.6 and 51% (average 22%).

Measurements of RONO<sub>2</sub> in ambient aerosol have so far mainly been performed from filter samples and therefore with low time resolution. Detection of RONO<sub>2</sub> is usually achieved via detection of the -ONO<sub>2</sub> group either optically or by mass spectrometry, with recent developments made toward high time resolution detection of RONO<sub>2</sub> [Ayes *et al.*, 2015; Hao *et al.*, 2014; Rollins *et al.*, 2012; Schlag *et al.*, 2015; Sun *et al.*, 2012; Xu *et al.*, 2015a; Xu *et al.*, 2015b]. Comparing with literature data obtained mainly from offline and online aerosol analysis in individual case studies in the US and Europe [Brown and Stutz, 2012; Fry *et al.*, 2013; Rollins *et al.*, 2012; Setyan *et al.*, 2012; Xu *et al.*, 2015a; Xu *et al.*, 2015b], we find a high contribution of organic nitrates to total organic PM1. For example, recent analysis of data from the southeast U.S. find that organic nitrates contribute 5 to 12% to organic aerosol in summer [Xu *et al.*, 2015a; Xu *et al.*, 2015b], whereas the results here imply a contribution of organic nitrates to European PM1 organics of on average 46%. Exploiting the high time resolution of AMS measurements, for the first time it is shown in an extended data set (spanning a continent and multiple seasons) that the concentration of organic nitrate is maximum during the nighttime for 12 of the 19 data sets with pOrgNO<sub>3</sub> above detection limit (see Figures S4–S7). Recent modeling studies suggest that at the global scale, 13% of the biogenic SOA production originates from NO<sub>3</sub> oxidation [Pye *et al.*, 2010]. For summer time in the USA up to 3.35 μg m<sup>-3</sup> of SOA is formed from NO<sub>3</sub> oxidation of biogenic VOC, equivalent to a doubling of the terpene SOA in some regions,

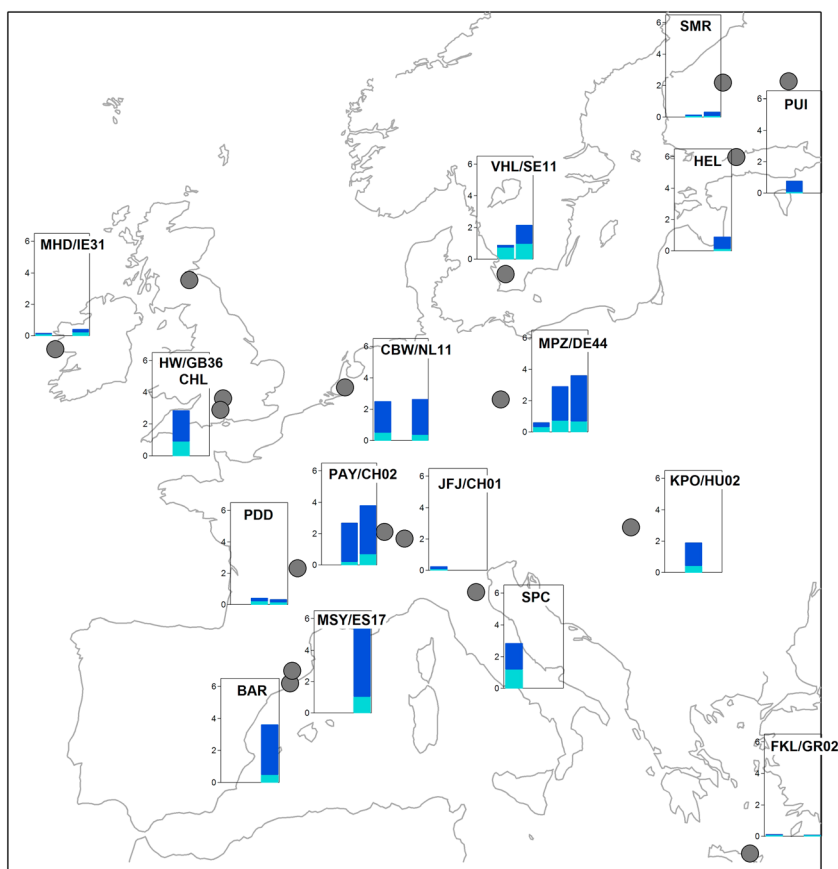


**Figure 3.** Map overview of particulate inorganic nitrate (pInNO<sub>3</sub>, dark blue) and particulate organic nitrate (pOrgNO<sub>3</sub>, cyan) mass concentrations ( $\mu\text{g m}^{-3}$ ) as observed during the EUCAARI/EMEP intensive measurement periods in May 2008 (left bar), October 2008 (middle), and March 2009 (right). Organic nitrate mass concentrations are high in all urban and rural sites and reach maximum concentrations during the night (see supporting information for detailed time series plots, diurnals, and station abbreviations).

when considering the formation by NO<sub>3</sub> oxidation [Pye *et al.*, 2010]. Similarly, our simulations for Europe (details see supporting information) show an increase of SOA by 50 to 70% when considering SOA formation by NO<sub>3</sub> oxidation with maximum ground level concentrations of SOA from NO<sub>3</sub> oxidation in the range of 2 to 4  $\mu\text{g m}^{-3}$  in May 2008 (Figure 4).

As shown in Figure S8 and summarized in Table S3, EURAD-IM performed well in predicting organic PM<sub>1</sub> concentrations with an overall normalized mean error (NME) of 53% and a normalized mean bias (NMB) of -45%. It reproduces observed daily mean organic aerosol concentration within a factor of 10 for 98% of all data points and within a factor of 2 for 57% of all data points. On the other hand, EURAD underestimates SOA from NO<sub>3</sub> when compared with observed pOrgNO<sub>3</sub> with a normalized mean bias (NMB) of -50% and an overall

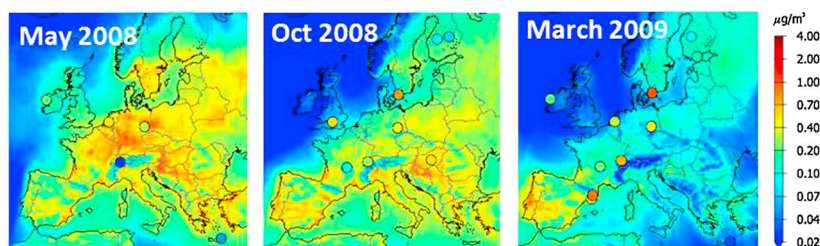


**Figure 4.** EURAD monthly mean concentration fields for SOA from NO<sub>3</sub> oxidation together with observed concentrations of pOrgNO<sub>3</sub> (colored circles) for May 2008 (left), October 2008 (middle), and March 2009 (right), respectively.

normalized mean error (NME) of 85%. This is worth mentioning specifically since pOrgNO<sub>3</sub> as measured here represents only a small fraction of SOA from NO<sub>3</sub> for two reasons. First, the pOrgNO<sub>3</sub> concentration reported is measure of the mass concentration of the nitrate functionality only of RONO<sub>2</sub>. Second, the reaction of VOC with NO<sub>3</sub> also leads to the formation of products without NO<sub>3</sub> functionality, therefore not covered in the measurement assignment of pOrgNO<sub>3</sub> to SOA from NO<sub>3</sub> oxidation. This under estimation is likely due to overall uncertainties in the modeling of SOA. The model treats NO<sub>3</sub> oxidation of anthropogenic VOCs (Cresole and other hydroxy substituted aromatics, terminal, and internal alkenes) and biogenic VOCs (isoprene,  $\alpha$ -pinene, and other cyclic terpenes with one double bond, d-limonene, and other cyclic diene-terpenes) according to the RACM [Stockwell *et al.*, 1997] chemistry mechanism. First and foremost, emission strengths of these VOCs are highly uncertain. Especially, the estimation of biogenic VOC emissions is critical due to a lack of detailed information about the type of plant cover. Further uncertainties may be introduced by the lumping applied to chemical species in the RACM chemistry mechanism and by the simplifying assumption that SOA formation from NO<sub>3</sub> oxidation for all biogenic VOC can be parameterized according to results obtained from  $\alpha$ -pinene, limonene, and isoprene [Li *et al.*, 2013]. This assumption is a consequence of the limited number of experimental studies available. It should also be mentioned that the comparison shows a larger NMB for the March 2009 data set (−74%) potentially indicating the presence of additional sources of pOrgNO<sub>3</sub> beyond oxidation of VOC with NO<sub>3</sub>. Due to the coarse model resolution (15 km) some of the measurement sites are not representative for the grid box used for comparison. Especially, a comparison of measurement data and model results is highly uncertain for the stations Jungfraujoch and Puy de Dome because of their exposed position. Also, in particular, the pOrgNO<sub>3</sub> measured at Vavihill, a continental background site with no local sources of pollution, situated in the southernmost part of Sweden, greatly exceeds modeled SOA from NO<sub>3</sub> (see also Figure 4). This potentially hints at additional sources for pOrgNO<sub>3</sub> at the Vavihill measurement site, potentially through influx of polluted air from continental Europe to the Nordic countries along a south-north transect. The inversion algorithm of EURAD-IM is currently designed as an inversion algorithm for gas phase [Elbern *et al.*, 2007]. Once the adjoint of SORGAM is available, it will be extended for SOA precursor emission estimation. Based on Moderate Resolution Imaging Spectroradiometer land use information, and higher horizontal resolution, the deficits can be addressed in a more systematic way. Furthermore, SORGAM improvements are expected taking recent experimental results on SOA formation due to reaction of  $\alpha$ -pinene and  $\beta$ -pinene with NO<sub>3</sub> into account [Boyd *et al.*, 2015; Nah *et al.*, 2016; Xu *et al.*, 2015a, 2015b]. Disregarding the underestimation of daily mean pOrgNO<sub>3</sub> concentrations at some measurement sites, the ability of the EURAD-IM to demonstrate qualitatively the daily cycle of pOrgNO<sub>3</sub> and the dilution tracer radon supports the assumption that nighttime NO<sub>3</sub> chemistry contributes significantly to the pOrgNO<sub>3</sub> production.

The spatial distribution and diurnal pattern of pOrgNO<sub>3</sub> indicate a gradient of concentration with high concentration found in source regions, i.e., regions with high-NO<sub>x</sub> emissions and during nighttime, and low concentrations in remote regions and during the day. Part of the diurnal pattern will be due to boundary layer dynamics, but the question remains to what extent the observed diurnal and regional variability is indicative of deposition losses, chemical reactions leading to fragmentation, or evaporative loss.

## 5. Implications and Conclusions

Across Europe a large fraction of the AMS measured nitrate is found to be organic, emphasizing the need to better understand sources and properties of particulate organic nitrates. The modeled continental distribution of SOA from NO<sub>3</sub> by the EURAD-IM supports the importance of NO<sub>3</sub> reactions during the night leading to SOA in regions with high-NO<sub>x</sub> emissions. It also shows the need for more extensive investigations of the chemistry and emissions leading to pOrgNO<sub>3</sub>.

Due to the lifetime of gas-phase RONO<sub>2</sub> with respect to photolysis (12–20 days), OH reactions (3–40 days), or thermal decomposition (up to months), some RONO<sub>2</sub> molecules may represent a temporary NO<sub>x</sub> reservoir [Aschmann *et al.*, 2011; Brown and Stutz, 2012; Nah *et al.*, 2016]; whereas, other organic molecules may be lost rapidly due to gas-phase deposition [Farmer *et al.*, 2006; Lee *et al.*, 2016] or particle phase hydrolysis [Boyd *et al.*, 2015; Liu *et al.*, 2012]. Particulate RONO<sub>2</sub> could serve as source of NO<sub>x</sub> in regions without major anthropogenic NO<sub>x</sub> sources due to repartitioning of organic nitrates [Fry *et al.*, 2013] into the gas phase or release of NO<sub>x</sub> following heterogeneous reactions [Liu *et al.*, 2012]. On the other hand, recent laboratory-based

observations indicate that  $\text{RONO}_2$  might irreversibly condense on SOA [Perraud et al., 2012]. This would imply that particulate  $\text{RONO}_2$  can serve as an important  $\text{NO}_x$  sink.

Little is known about the properties of particulate organic nitrate with respect to both health risks and climate effects. Direct climate effects of organic nitrates may arise from their absorbing properties, which could be significantly higher than for SOA formed from OH or  $\text{O}_3$  initiated oxidation [Moise et al., 2015]. Similar to other organic semivolatile vapors, organic nitrates can be expected to cocondense with water when aerosol particles activate to cloud droplets [Topping et al., 2013], impacting aerosol indirect effects on climate. At the median level, for all sites studied here organic nitrates suggest a comparable contribution to increasing kappa as nitric acid (see supporting information and Figure S9) [Barley et al., 2011; Topping and McFiggans, 2012]. Such effects of organic nitrate condensation onto activating aerosol particles should be considered alongside those from nitric acid in increasing the number concentration of cloud droplets. Through its formation by  $\text{NO}_3$  oxidation, and thereby its strong relation to anthropogenic  $\text{NO}_x$  emissions, particulate organic nitrates will be directly affected by  $\text{NO}_x$  emission controls [Rollins et al., 2012] with the potential to decrease specifically nighttime  $\text{PM}_{10}$  burdens in urban and rural sites in Europe.

#### Acknowledgments

This work was supported by the European Commission through EUCAARI IP (contract 036833-2) and PEGASOS (FP7-ENV-2010-265148). Transnational access to the measurement sites in Cabauw and Kpuszta was supported by ACCENT. Measurements were further funded by the following national sources: the UK Department for Environment, Food and Rural Affairs (Defra), the German Federal Environment Agency (Umweltbundesamt, grants 351 03 031 and 351 01 038, and UFOPLAN grant 3703 43 200), the Swiss Federal Office for the Environment, and NOAA NA13OAR4310063 and EPA STAR 83587701-0.

#### References

- Ackermann, I. J., H. Hass, M. Memmesheimer, A. Ebel, F. S. Binkowski, and U. Shankar (1998), Modal aerosol dynamics model for Europe: Development and first applications, *Atmos. Environ.*, *32*(17), 2981–2999.
- Allan, J. D., et al. (2004), A generalised method for the extraction of chemically resolved mass spectra from aerodyne aerosol mass spectrometer data, *J. Aerosol Sci.*, *35*(7), 909–922.
- Aschmann, S. M., E. C. Tuazon, J. Arey, and R. Atkinson (2011), Products of the OH radical-initiated reactions of 2-propyl nitrate, 3-methyl-2-butyl nitrate and 3-methyl-2-pentyl nitrate, *Atmos. Environ.*, *45*(9), 1695–1701.
- Ayres, B. R., et al. (2015), Organic nitrate aerosol formation via  $\text{NO}_3$  + biogenic volatile organic compounds in the southeastern United States, *Atmos. Chem. Phys.*, *15*(23), 13,377–13,392.
- Barley, M. H., D. Topping, D. Lowe, S. Utembe, and G. McFiggans (2011), The sensitivity of secondary organic aerosol (SOA) component partitioning to the predictions of component properties—Part 3: Investigation of condensed compounds generated by a near-explicit model of VOC oxidation, *Atmos. Chem. Phys.*, *11*(24), 13,145–13,159.
- Boyd, C. M., J. Sanchez, L. Xu, A. J. Eugene, T. Nah, W. Y. Tuet, M. I. Guzman, and N. L. Ng (2015), Secondary organic aerosol formation from the  $\beta$ -pinene +  $\text{NO}_3$  system: Effect of humidity and peroxy radical fate, *Atmos. Chem. Phys.*, *15*(13), 7497–7522.
- Brown, S. S., and J. Stutz (2012), Nighttime radical observations and chemistry, *Chem. Soc. Rev.*, *41*(19), 6405–6447.
- Brown, S. S., et al. (2009), Nocturnal isoprene oxidation over the northeast United States in summer and its impact on reactive nitrogen partitioning and secondary organic aerosol, *Atmos. Chem. Phys.*, *9*(9), 3027–3042.
- Bruns, E. A., V. r. Perraud, A. Zelenyuk, M. J. Ezell, S. N. Johnson, Y. Yu, D. Imre, B. J. Finlayson-Pitts, and M. L. Alexander (2010), Comparison of FTIR and particle mass spectrometry for the measurement of particulate organic nitrates, *Environ. Sci. Technol.*, *44*(3), 1056–1061.
- Canagaratna, M. R., et al. (2007), Chemical and microphysical characterization of ambient aerosols with the aerodyne aerosol mass spectrometer, *Mass Spectrom. Rev.*, *26*(2), 185–222.
- Carbone, S., et al. (2014), Wintertime aerosol chemistry in sub-Arctic urban air, *Aerosol Sci. Technol.*, *48*(3), 313–323.
- Chervenkov, H., and H. Jakobs (2011), Dust storm simulation with regional air quality model—Problems and results, *Atmos. Environ.*, *45*(24), 3965–3976.
- Crippa, M., et al. (2013), Organic aerosol components derived from 25 AMS datasets across Europe using a newly developed ME-2 based source apportionment strategy, *Atmos. Chem. Phys. Discuss.*, *13*(9), 23,325–23,371.
- Dall'Osto, M., et al. (2010), Aerosol properties associated with air masses arriving into the North East Atlantic during the 2008 Mace Head EUCAARI intensive observing period: An overview, *Atmos. Chem. Phys.*, *10*(17), 8413–8435.
- DeCarlo, P. F., et al. (2006), Field-deployable, high-resolution, time-of-flight aerosol mass spectrometer, *Anal. Chem.*, *78*(24), 8281–8289.
- Elbern, H., A. Strunk, H. Schmidt, and O. Talagrand (2007), Emission rate and chemical state estimation by 4-dimensional variational inversion, *Atmos. Chem. Phys.*, *7*(14), 3749–3769.
- Farmer, D. K., P. J. Wooldridge, and R. C. Cohen (2006), Application of thermal-dissociation laser induced fluorescence (TD-LIF) to measurement of  $\text{HNO}_3$ , Sigma alkyl nitrates, Sigma peroxy nitrates, and  $\text{NO}_2$  fluxes using eddy covariance, *Atmos. Chem. Phys.*, *6*(11), 3471–3486.
- Farmer, D. K., A. Matsunaga, K. S. Docherty, J. D. Surratt, J. H. Seinfeld, P. J. Ziemann, and J. L. Jimenez (2010), Response of an aerosol mass spectrometer to organonitrates and organosulfates and implications for atmospheric chemistry, *Proc. Natl. Acad. Sci. U.S.A.*, *107*(15), 6670–6675.
- Frey, E. J., K. Sellegri, F. Canonaco, J. Boulon, M. Hervo, R. Weigel, J. M. Pichon, A. Colomb, A. S. H. Prévôt, and P. Laj (2011), Seasonal variations in aerosol particle composition at the puy-de-Dôme research station in France, *Atmos. Chem. Phys.*, *11*(24), 13,047–13,059.
- Fry, J. L., et al. (2009), Organic nitrate and secondary organic aerosol yield from  $\text{NO}_3$  oxidation of  $\beta$ -pinene evaluated using a gas-phase kinetics/aerosol partitioning model, *Atmos. Chem. Phys.*, *9*(4), 1431–1449.
- Fry, J. L., et al. (2011), SOA from limonene: Role of  $\text{NO}_3$  in its generation and degradation, *Atmos. Chem. Phys.*, *11*(8), 3879–3894.
- Fry, J. L., et al. (2013), Observations of gas- and aerosol-phase organic nitrates at BEACHON-RoMBAS 2011, *Atmos. Chem. Phys.*, *13*(17), 8585–8605.
- Fry, J. L., et al. (2014), Secondary organic aerosol formation and organic nitrate yield from  $\text{NO}_3$  oxidation of biogenic hydrocarbons, *Environ. Sci. Technol.*, *48*(20), 11,944–11,953.
- Guenther, A. B., X. Jiang, C. L. Heald, T. Sakulyanontvittaya, T. Duhl, L. K. Emmons, and X. Wang (2012), The Model of Emissions of Gases and Aerosols from Nature version 2.1 (MEGAN 2.1): An extended and updated framework for modeling biogenic emissions, *Geosci. Model Dev.*, *5*(6), 1471–1492.
- Hallquist, M., et al. (2009), The formation, properties and impact of secondary organic aerosol: Current and emerging issues, *Atmos. Chem. Phys.*, *9*(14), 5155–5236.



- Hao, L. Q., et al. (2014), Atmospheric submicron aerosol composition and particulate organic nitrate formation in a boreal forestland–urban mixed region, *Atmos. Chem. Phys.*, *14*(24), 13,483–13,495.
- Hildebrandt, L., E. Kostenidou, V. A. Lanz, A. S. H. Prevot, U. Baltensperger, N. Mihalopoulos, A. Laaksonen, N. M. Donahue, and S. N. Pandis (2011), Sources and atmospheric processing of organic aerosol in the Mediterranean: Insights from aerosol mass spectrometer factor analysis, *Atmos. Chem. Phys.*, *11*(23), 12,499–12,515.
- Jayne, J. T., D. C. Leard, X. F. Zhang, P. Davidovits, K. A. Smith, C. E. Kolb, and D. R. Worsnop (2000), Development of an aerosol mass spectrometer for size and composition analysis of submicron particles, *Aerosol Sci. Technol.*, *33*(1–2), 49–70.
- Kulmala, M., et al. (2011), General overview: European Integrated Project on Aerosol Cloud Climate and Air Quality Interactions (EUCAARI)—Integrating aerosol research from nano to global scales, *Atmos. Chem. Phys.*, *11*(24), 13,061–13,143.
- Lanz, V. A., et al. (2010), Characterization of aerosol chemical composition with aerosol mass spectrometry in Central Europe: An overview, *Atmos. Chem. Phys.*, *10*(21), 10,453–10,471.
- Lee, B. H., et al. (2016), Highly functionalized organic nitrates in the southeast United States: Contribution to secondary organic aerosol and reactive nitrogen budgets, *Proc. Natl. Acad. Sci. U.S.A.*, *113*(6), 1516–1521.
- Li, Y. P., H. Elbern, K. D. Lu, E. Friese, A. Kiendler-Scharr, T. F. Mentel, X. S. Wang, A. Wahner, and Y. H. Zhang (2013), Updated aerosol module and its application to simulate secondary organic aerosols during IMPACT campaign May 2008, *Atmos. Chem. Phys.*, *13*(13), 6289–6304.
- Liu, S., J. E. Shilling, C. Song, N. Hiranuma, R. A. Zaveri, and L. M. Russell (2012), Hydrolysis of organonitrate functional groups in aerosol particles, *Aerosol Sci. Technol.*, *46*(12), 1359–1369.
- Mensah, A. A., R. Holzinger, R. Otjes, A. Trimborn, T. F. Mentel, H. ten Brink, B. Henzing, and A. Kiendler-Scharr (2012), Aerosol chemical composition at Cabauw, The Netherlands as observed in two intensive periods in May 2008 and March 2009, *Atmos. Chem. Phys.*, *12*(10), 4723–4742.
- Minguillón, M. C., et al. (2011), Fossil versus contemporary sources of fine elemental and organic carbonaceous particulate matter during the DAURE campaign in northeast Spain, *Atmos. Chem. Phys.*, *11*(23), 12,067–12,084.
- Mohr, C., et al. (2012), Identification and quantification of organic aerosol from cooking and other sources in Barcelona using aerosol mass spectrometer data, *Atmos. Chem. Phys.*, *12*(4), 1649–1665.
- Moise, T., J. M. Flores, and Y. Rudich (2015), Optical properties of secondary organic aerosols and their changes by chemical processes, *Chem. Rev.*, *115*(10), 4400–4439.
- Monteiro, A., et al. (2012), Investigating a high ozone episode in a rural mountain site, *Environ. Pollut.*, *162*, 176–189.
- Nah, T., J. Sanchez, C. M. Boyd, and N. L. Ng (2016), Photochemical aging of  $\alpha$ -pinene and  $\beta$ -pinene secondary organic aerosol formed from nitrate radical oxidation, *Environ. Sci. Technol.*, *50*(1), 222–231.
- Paglione, M., et al. (2014), Identification of humic-like substances (HULIS) in oxygenated organic aerosols using NMR and AMS factor analyses and liquid chromatographic techniques, *Atmos. Chem. Phys.*, *14*(1), 25–45.
- Pankow, J. F., and W. E. Asher (2008), SIMPOL.1: A simple group contribution method for predicting vapor pressures and enthalpies of vaporization of multifunctional organic compounds, *Atmos. Chem. Phys.*, *8*(10), 2773–2796.
- Perraud, V., et al. (2012), Nonequilibrium atmospheric secondary organic aerosol formation and growth, *Proc. Natl. Acad. Sci. U.S.A.*, *109*(8), 2836–2841.
- Pikridas, M., et al. (2010), The Finokalia Aerosol Measurement Experiment - 2008 (FAME-08): An overview, *Atmos. Chem. Phys.*, *10*(14), 6793–6806.
- Poulain, L., G. Spindler, W. Birmili, C. Plass-Dülmer, A. Wiedensohler, and H. Herrmann (2011), Seasonal and diurnal variations of particulate nitrate and organic matter at the IFT research station Melpitz, *Atmos. Chem. Phys.*, *11*(24), 12,579–12,599.
- Pouliot, G., T. Pierce, H. D. van der Gon, M. Schaap, M. Moran, and U. Nopmngcol (2012), Comparing emission inventories and model-ready emission datasets between Europe and North America for the AQMEII project, *Atmos. Environ.*, *53*, 4–14.
- Pye, H. O. T., A. W. H. Chan, M. P. Barkley, and J. H. Seinfeld (2010), Global modeling of organic aerosol: The importance of reactive nitrogen ( $\text{NO}_x$  and  $\text{NO}_3$ ), *Atmos. Chem. Phys.*, *10*(22), 11,261–11,276.
- Rollins, A. W., et al. (2009), Isoprene oxidation by nitrate radical: Alkyl nitrate and secondary organic aerosol yields, *Atmos. Chem. Phys.*, *9*(18), 6685–6703.
- Rollins, A. W., et al. (2012), Evidence for  $\text{NO}_x$  control over nighttime SOA formation, *Science*, *337*(6099), 1210–1212.
- Saarikoski, S., et al. (2012), Chemical characterization of springtime submicrometer aerosol in Po Valley, Italy, *Atmos. Chem. Phys. Discuss.*, *12*(3), 8269–8318.
- Schell, B., I. J. Ackermann, H. Hass, F. S. Binkowski, and A. Ebel (2001), Modeling the formation of secondary organic aerosol within a comprehensive air quality model system, *J. Geophys. Res.*, *106*(D22), 28,275–28,293.
- Schlag, P., A. Kiendler-Scharr, M. J. Blom, F. Canonaco, J. S. Henzing, M. M. Moerman, A. S. H. Prévôt, and R. Holzinger (2015), Aerosol source apportionment from 1 year measurements at the CESAR tower at Cabauw, NL, *Atmos. Chem. Phys. Discuss.*, *2015*, 35,117–35,155.
- Setyan, A., et al. (2012), Characterization of submicron particles influenced by mixed biogenic and anthropogenic emissions using high-resolution aerosol mass spectrometry: Results from CARES, *Atmos. Chem. Phys.*, *12*(17), 8131–8156.
- Spracklen, D. V., et al. (2011), Aerosol mass spectrometer constraint on the global secondary organic aerosol budget, *Atmos. Chem. Phys.*, *11*(23), 12,109–12,136.
- Stockwell, W. R., F. Kirchner, M. Kuhn, and S. Seefeld (1997), A new mechanism for regional atmospheric chemistry modeling, *J. Geophys. Res.*, *102*(D22), 25,847–25,879.
- Sun, Y. L., Q. Zhang, J. J. Schwab, T. Yang, N. L. Ng, and K. L. Demerjian (2012), Factor analysis of combined organic and inorganic aerosol mass spectra from high resolution aerosol mass spectrometer measurements, *Atmos. Chem. Phys.*, *12*(18), 8537–8551.
- Szidat, S., T. M. Jenk, H.-A. Synal, M. Kalberer, L. Wacker, I. Hajdas, A. Kasper-Giebl, and U. Baltensperger (2006), Contributions of fossil fuel, biomass-burning, and biogenic emissions to carbonaceous aerosols in Zurich as traced by  $^{14}\text{C}$ , *J. Geophys. Res.*, *111*(D7), D07206, doi:10.1029/2005JD006590.
- Topping, D., P. Connolly, and G. McFiggans (2013), Cloud droplet number enhanced by co-condensation of organic vapours, *Nat. Geosci.*, *6*(6), 443–446.
- Topping, D. O., and G. McFiggans (2012), Tight coupling of particle size, number and composition in atmospheric cloud droplet activation, *Atmos. Chem. Phys.*, *12*(7), 3253–3260.
- Ulbrich, I. M., M. R. Canagaratna, Q. Zhang, D. R. Worsnop, and J. L. Jimenez (2009), Interpretation of organic components from Positive Matrix Factorization of aerosol mass spectrometric data, *Atmos. Chem. Phys.*, *9*(9), 2891–2918.
- Weber, R. J., et al. (2007), A study of secondary organic aerosol formation in the anthropogenic-influenced southeastern United States, *J. Geophys. Res.*, *112*, doi:10.1029/2007JD008408.
- Winer, A. M., R. Atkinson, and J. N. Pitts (1984), Gaseous nitrate radical: Possible nighttime atmospheric sink for biogenic organic compounds, *Science*, *224*(4645), 156–159.

- Xu, L., S. Suresh, H. Guo, R. J. Weber, and N. L. Ng (2015a), Aerosol characterization over the southeastern United States using high-resolution aerosol mass spectrometry: Spatial and seasonal variation of aerosol composition and sources with a focus on organic nitrates, *Atmos. Chem. Phys.*, *15*(13), 7307–7336.
- Xu, L., et al. (2015b), Effects of anthropogenic emissions on aerosol formation from isoprene and monoterpenes in the southeastern United States, *Proc. Natl. Acad. Sci. U.S.A.*, *112*(1), 37–42.
- Zhang, L., J. R. Brook, and R. Vet (2003), A revised parameterization for gaseous dry deposition in air-quality models, *Atmos. Chem. Phys.*, *3*(6), 2067–2082.
- Zhang, Q., et al. (2007), Ubiquity and dominance of oxygenated species in organic aerosols in anthropogenically-influenced Northern Hemisphere midlatitudes, *Geophys. Res. Lett.*, *34*, doi:10.1029/2007GL029979.